

## Elastic constants and anisotropy of forsterite at high pressure

Cesar da Silva

Dept. of Chemical Engineering and Materials Science, and Minnesota Supercomputer Institute  
University of Minnesota

Lars Stixrude

School of Earth and Atmospheric Sciences, Georgia Institute of Technology

Renata M. Wentzcovitch

Dept. of Chemical Engineering and Materials Science, and Minnesota Supercomputer Institute  
University of Minnesota

**Abstract.** We have determined from first principles the athermal elastic constant tensor of  $\text{Mg}_2\text{SiO}_4$  forsterite with the plane wave pseudopotential method over a wide range of pressure (0-100 GPa) that encompasses the full range over which forsterite has been observed experimentally. The computed elastic constants are in excellent agreement with experimental data up to the maximum pressure of the experiments (16 GPa). We calculate the single-crystal elastic anisotropy from the elastic constants. We find that the anisotropy is strong (azimuthal P- and S-wave anisotropy: 25 % and 20 %, respectively, polarization anisotropy: 15 %), in agreement with experiment, and that it depends weakly on pressure over the range 0-25 GPa, in contrast to the behavior of other silicates and oxides.

### Introduction

As the most abundant mineral species in the upper mantle, the elastic properties of forsterite play a major role in our understanding of the composition of this region. Moreover, the large elastic anisotropy exhibited by forsterite make it a potential marker of mantle flow through seismological determinations of mantle anisotropy.

The elastic constants of forsterite [Zha *et al.*, 1996] and olivine [10 % fayalite, Zaig *et al.*, 1993; Abramson *et al.*, 1997] have recently been determined experimentally at mantle pressures. Isotropically averaged velocities based on these data have been compared seismic observations. However, the anisotropy of this mineral at high pressure has not been discussed. This is a particularly important issue since seismic anisotropy is generally interpreted in terms of the zero pressure elastic constants of olivine, not necessarily representative of the anisotropy of this mineral at typical upper mantle conditions. Moreover, experiments on different olivines have yielded significantly different results. It is unclear to what extent these discrepancies are due to differences in experimental technique, or to real differences in composition.

To address these issues, we have determined the structure, equation of state, and elastic constants of forsterite over a wide pressure range (0-100 GPa) which extends well beyond that of the upper mantle. The advantages of exploring a pressure interval much broader than that of the olivine stability field ( $P < 14$  GPa) are that 1) it serves to clarify the pressure dependence of the elastic constants at large finite strains 2) it permits contact between theory and the full pressure range over which this mineral has been observed experimentally (up to  $P = 70$  GPa) [Andraut *et al.*, 1995; Ahrens *et al.*, 1982].

### Computational Methods

We have used a first principles variable cell shape molecular dynamics strategy [Wentzcovitch *et al.*, 1993] to obtain the ground state configuration of strained and unstrained structures at arbitrary pressures. This technique combines density functional theory, in principle an exact theory of the electronic ground state energy and density with a classical molecular dynamics strategy [Wentzcovitch, 1991] which allows for efficient minimization of forces and stresses through simultaneous relaxation of all structural parameters. This type of technique has been applied to several types of solids, including mantle silicates [Wentzcovitch *et al.*, 1993; Wentzcovitch *et al.*, 1995; Karki *et al.*, 1997b] and forsterite [Brodholt *et al.*, 1996; Wentzcovitch and Stixrude, 1997]. The calculations are performed within the Local Density Approximation (LDA) [Ceperley and Alder, 1980].

We used the same norm-conserving Troullier-Martins [1991] pseudopotentials of our previous study of the compression of forsterite [Wentzcovitch and Stixrude, 1997]. The number of plane-waves is set by the energy cutoff (70 Ry) leading to 8500 basis functions per  $\text{Mg}_2\text{SiO}_4$  unit. The Brillouin zone was sampled on a  $2 \times 2 \times 2$  k-point mesh, but since the structural optimizations conserved the space group symmetry the effective number was reduced to 1 and 4 k-points in the irreducible wedge for lattices under uniaxial and shear strains, respectively.

To determine the elastic constants at a given pressure, we first determine the equilibrium structure of the 28-atom orthorhombic unit cell by minimizing the Hellman-Feynman forces and stresses [Nielsen and Martin, 1985] acting respectively on the nuclei and the lat-

tice parameters. The elastic constants are then determined by applying strains and calculating the resulting stress tensor. Because strains couple to vibrational modes the atomic positions are re-optimized in the strained configuration. Three uniaxial and one shear (triclinic) strain are used to calculate the nine elastic moduli. We perform calculations for negative and positive values of each strain (magnitude 1 %), in order to determine precisely the value of the elastic constants in the appropriate limit of zero strain. This method has been applied previously to the determination of the elastic constants in silicates and oxides [Wentzcovitch *et al.*, 1993; Karaki *et al.*, 1997a, 1997b].

## Results

The computed elastic constants and their pressure dependencies compare favorably with experimental measurements (Fig. 1, Table 1). The theoretical elastic constants are generally higher, as expected: experimental temperatures (300 K) are expected to lower elastic constants relative to their athermal values by several percent. Remaining discrepancies between theory and experiment (the largest deviation is 11 % in the case of  $c_{11}$ ) are attributed to the LDA and to the particular pseudopotential for magnesium used here [Kiefer, Stixrude, and Wentzcovitch, submitted], which causes the zero pressure lattice parameters to be underestimated [by 2 %, Wentzcovitch and Stixrude, 1997].

Elastic constants are found to increase monotonically and slightly sub-linearly with pressure,  $P$ , except for those  $c_{ij}$  for which  $i = j > 3$ :  $c_{55}$  and  $c_{66}$  decrease with increasing pressure for  $P > 40$  and  $P > 90$  GPa respectively. This behavior suggests that forsterite may undergo an elastic instability at high pressure: a finite strain extrapolation of our results implies that  $c_{55}$  vanishes at 173 GPa. Experiments also show a non-linear pressure dependence of  $c_{55}$  [Abramson *et al.*, 1997], although the non-linearity is much stronger than that found here, or in experiments on forsterite [Zha *et al.*, 1996]. The stronger non-linearity found experimentally for the iron-bearing sample suggests that iron may substantially affect the pressure dependence of  $c_{55}$ .

We represent our results by an expansion in the Eulerian finite strain,  $f = 1/2[(V/V_0)^{-2/3} - 1]$ ,

$$c_{ij} + P\Delta_{ij} = (1 + 2f)^{5/2}(a_2 + a_3f + \frac{1}{2}a_4f^2 + \dots) \quad (1)$$

$$a_2 = c_{ij0} \quad (2)$$

$$a_3 = 3K_0(c'_{ij0} + \Delta_{ij}) - 7a_2 \quad (3)$$

$$a_4 = 9K_0^2c''_{ij0} - 3K_0'(a_3 - 7a_2) + 16a_3 - 49a_2 \quad (4)$$

where the contracted Voigt notation is used, subscript 0 indicates values at zero pressure, primes indicate pressure derivatives,  $V$  is the volume,  $K$  the bulk modulus and  $\Delta_{ij} = -3$  if  $i = j \leq 3$ , and  $-1$  otherwise [Davies, 1974]. We found that the finite strain expansion converged rapidly: third-order expansions ( $a_4 = 0$ ) were sufficient, except for the highly non-linear pressure dependence displayed by  $c_{44}$ ,  $c_{55}$ , and  $c_{66}$  for which we used a fourth order expansion (Table 1, Fig. 1).

The compressional (P) and shear (S) wave velocities of isotropic aggregates calculated from our elastic constants (Voigt-Reuss-Hill average) agree with experimental determinations to within 1 % (Fig. 2). The aggregate velocities show a slightly sub-linear dependence on pressure over the range of the upper mantle, which is also seen experimentally [Zaug *et al.*, 1993; Li *et al.*, 1996]. For pressures beyond those of the upper mantle,  $V_S$  decreases with increasing pressure ( $P > 60$  GPa), largely due to the non-linear dependence of  $c_{44}$ ,  $c_{55}$ , and  $c_{66}$ .

We find that the anisotropy of single-crystal forsterite depends weakly on pressure. Solutions to the Cristoffel equation using our elastic constants show that the directional dependence of P- and S-wave velocities, and the differences between the two S-wave polarizations are qualitatively similar between 0 and 25 GPa. The fastest direction for P-wave propagation remains [100] and directions approximately  $45^\circ$  to the  $a$ -axis remain the direction of fastest S-wave propagation and maximum difference between S-wave polarizations. The magnitude of the anisotropy changes by less than 5 % between 0 and 25 GPa; values representative of the pressure regime of the upper mantle are 25 % and 20 %, respectively, for the azimuthal anisotropy of P- and S-waves and 15 % for the polarization anisotropy (Fig. 3). Theory and experiment agree to within 5 %, although experimentally, there appears to be an initial decrease

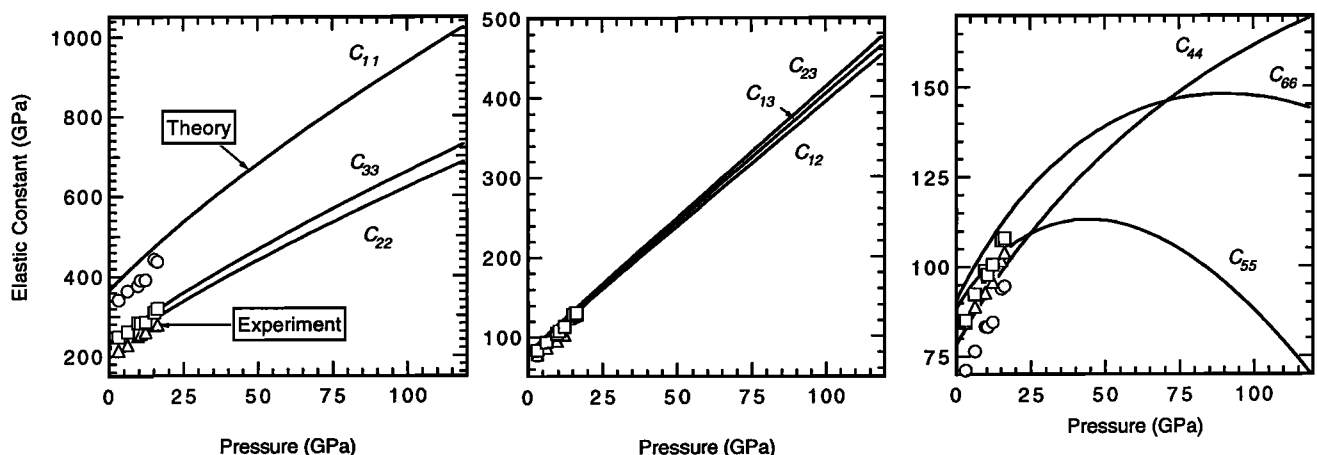


**Figure 1.** Computed elastic constants of forsterite. Lines are Eulerian finite strain fits with parameters given in Table 1. Experimental results of Zha *et al.* [1996] shown as symbols.

**Table 1.** Moduli,  $M_0$ , and their first and second pressure derivatives  $M'_0$ ,  $M''_0$  at zero pressure as determined from theory and experiment.

	Theory			Experiment		
	$M_0$ (GPa)	$M'_0$	$M''_0$ (GPa <sup>-1</sup> )	$M_0$ (GPa) <sup>1</sup>	$M'_0$	$M''_0$ (GPa <sup>-1</sup> ) <sup>2</sup>
$c_{11}$	367	7.68	(-0.085)	328.4	8.47, 7.22	-0.047
$c_{22}$	220	5.30	(-0.048)	199.8	6.56, 5.42	-0.051
$c_{33}$	233	5.61	(-0.052)	235.3	6.38, 5.57	-0.094
$c_{12}$	77.8	3.38	(-0.027)	63.9	4.67, 3.59	-0.009
$c_{13}$	79.3	3.46	(-0.027)	68.8	4.84, 3.62	-0.072
$c_{23}$	80.6	3.54	(-0.028)	73.8	4.11, 2.94	+0.077
$c_{44}$	78.4	1.53	-0.019	65.15	2.12, 2.01	-0.071
$c_{55}$	88.7	1.34	-0.028	81.20	1.66, 1.46	-0.021
$c_{66}$	90.8	1.69	-0.027	80.88	2.37, 2.16	-0.025
$K$	140.9	4.32		128.6	5.37, 4.19	
$\mu$	88.7	1.44		81.1	1.80, 1.4 <sup>3</sup>	

References: 1, *Kumazawa and Anderson* [1969]; 2, *Yoneda and Morioka* [1992]; 3, *Zha et al.* [1996]. Experimental values for  $M_0$  are from 1 (first entry) and 2 (second entry) unless otherwise noted. Theoretical values in parentheses are from third order fits ( $a_4 = 0$ ). The theoretical values of  $K_0$  and  $K'_0$  are consistent with those determined from the equation of state [*Wentzcovitch and Stixrude*, 1997]:  $V_0 = 40.95 \text{ cm}^3 \text{ mol}^{-1}$ ,  $K_0 = 139.1 \text{ GPa}$ ,  $K'_0 = 4.46$ .

in shear-wave anisotropies which is not reproduced by the calculations. We note that, experimentally, temperature also has a relatively weak effect: anisotropies increase by 3-5 % between 300 and 1700 K [*Isaak et al.*, 1989].

**Discussion and Conclusions**

Comparison with the upper mantle shows that isotropically averaged P- and S-wave velocity profiles nearly parallel those of forsterite between 200 and 400 km depth, but are displaced downwards by 7 % and 13 %, respectively (Fig. 2). These results are consistent with the hypothesis that upper mantle mineralogy above 400 km depth is dominated by olivine [*Duffy et al.*, 1995]. The differences between our results and seismic observations can be accounted for by the presence of Fe in the mantle, which is expected to reduce velocities by

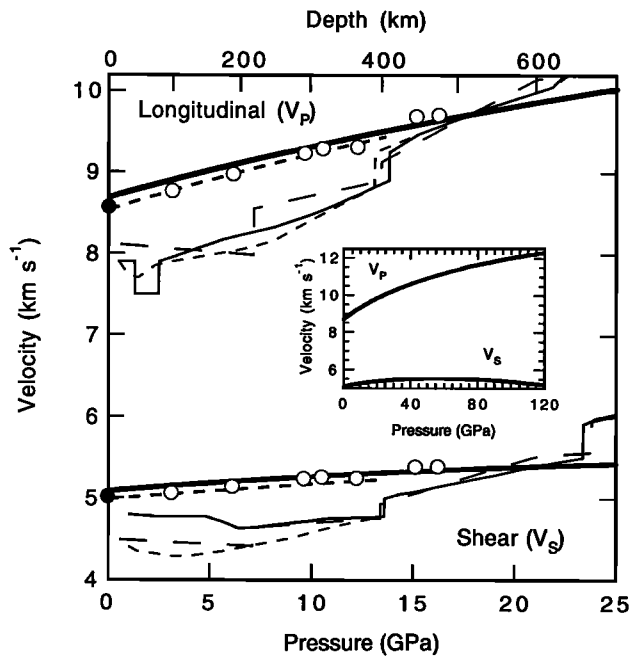


**Figure 2.** Voigt-Reuss-Hill average velocities determined from our theoretical elastic constants (lines) compared with experiment [*Zha et al.*, 1996, open symbols; *Kumazawa and Anderson*, 1969, closed symbols; *Li et al.*, 1996, heavy dashed lines], and P-wave seismological models GCA [*Walck*, 1984, dashed line] and CJF [*Walck*, 1985, solid line], S-wave models TNA and SNA [*Grand and Helmberger*, 1984, dashed and solid lines, respectively], and PREM [*Dziewonski and Anderson*, 1981, long dashed lines].

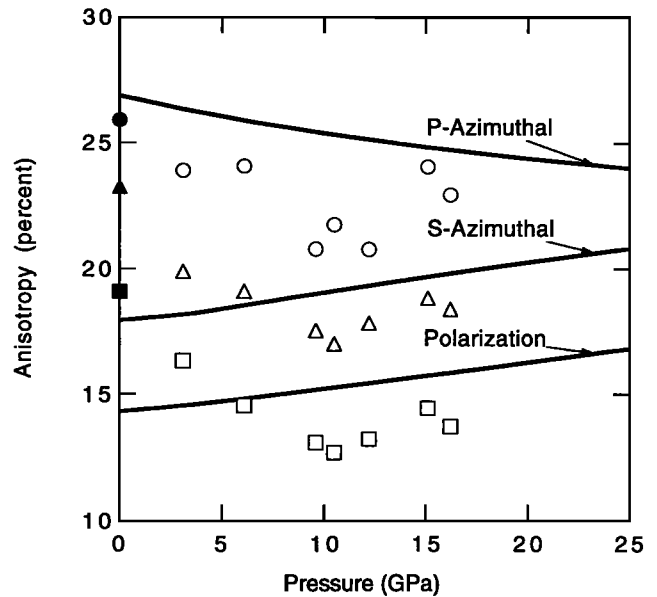


**Figure 3.** Computed anisotropy (lines) compared with that experimentally measured by *Zha et al.* [1996] (open symbols), and *Kumazawa and Anderson* [1969] (closed symbols): P-wave azimuthal (circles), S-wave azimuthal (triangles), polarization (squares).

2-3 %, and the high temperatures in the upper mantle, expected to reduce velocities by approximately 10 % relative to their athermal values [Kumazawa and Anderson, 1969; Isaak *et al.*, 1989]. The presence of other abundant phases such as pyroxene and garnet likely also contribute to the difference.

The weak pressure dependence of the elastic anisotropy in forsterite contrasts with the behavior of other oxides and silicates (Fig. 3). The anisotropy of MgSiO<sub>3</sub> perovskite increases by a factor of two over the pressure regime of the lower mantle, while the azimuthal S-wave anisotropy of periclase decreases from 16 % to zero between 0 and 20 GPa, before rising again to 59 % at 150 GPa [Karki *et al.*, 1997a, 1997b]. The weak pressure dependence of the anisotropy of forsterite is important because it supports the mineralogical basis for most previous interpretations of mantle anisotropy in terms of mantle flow. [Christensen and Salisbury, 1979; Tanimoto and Anderson, 1984]. These interpretations, which attribute anisotropy largely to flow-induced lattice preferred orientation of olivine dominated aggregates, have been primarily based on ambient or low pressure measurements of the elastic constants of olivine which, as we have shown, provide a good first order approximation to the anisotropy of olivine throughout the upper mantle.

Modern first principles methods are now capable of realistic predictions of the elastic constants of complex silicates such as forsterite. Although completely independent of experimental data, we have shown that these methods are able to reproduce even subtle features such as elastic anisotropy with good accuracy. We note that it is possible to extend these methods to high temperatures, although we have not done so here. Modern electronic structure theory thus promises an ideal complement to the experimental approach, and the ability to determine the elasticity and anisotropy of major constituents throughout the pressure regime of the earth's mantle.

**Acknowledgments.** This work supported by the National Science Foundation under grants EAR-9628199 (LPS) and EAR-9628042 (RMW), and by the Minnesota Supercomputer Institute.

## References

- Abramson, E. H., J. M. Brown, L. J. Slutsky, and J. Zaugg, The elastic constants of San Carlos olivine to 17 GPa, *J. Geophys. Res.*, **102**, 12253-12263, 1997.
- Ahrens, T. J., G. A. Lyzenga, and A. C. Mitchell, Temperatures induced by shock waves in minerals: applications to geophysics, *High Pressure Res. in Geophysics*, S. Akimoto and M. H. Manghnani (eds.), pp. 579-594, Center for Academic Publications, Tokyo, 1982.
- Andrault, D., M. A. Bouhifd, J. P. Itie, and P. Richet, Compression and amorphization of (Mg,Fe)<sub>2</sub>SiO<sub>4</sub> olivines: an x-ray diffraction study up to 70 GPa, *Phys. Chem. Minerals*, **22**, 99-107, 1995.
- Brodholt, J., A. Patel, and K. Refson, An ab initio study of the compressional behavior of forsterite, *Am. Mineral.*, **81**, 257-260, 1996.
- Ceperley, D. M., and B. J. Alder, Ground state of the electron gas by a stochastic method, *Phys. Rev. Lett.*, **45**, 566-569, 1980.
- Christensen, N. I. and M. H. Salisbury, Seismic anisotropy in the upper mantle: evidence from the Bay of Islands ophiolite complex, *J. Geophys. Res.*, **84**, 4601-4610, 1979.
- Davies, G. F. Effective elastic moduli under hydrostatic stress - I. quasiharmonic theory, *J. Phys. Chem. Solids*, **35**, 1513-1520, 1974.
- Duffy, T. S., C. S. Zha, R. T. Downs, H. K. Mao, et al., Elasticity of forsterite to 16 GPa and the composition of the upper mantle, *Nature*, **378**, 170-173, 1995.
- Grand, S. P. and D. V. Helmberger, Upper mantle shear structure of North America, *Geophys. J. Roy. Astr. Soc.*, **76**, 399-438, 1984.
- Isaak, D. G., O. L. Anderson, T. Goto, and I. Suzuki, Elasticity of single-crystal forsterite measured to 1700 K, *J. Geophys. Res.*, **94**, 5895-5906, 1989.
- Karki, B. B., L. Stixrude, S. J. Clark, M. C. Warren, G. J. Ackland, and J. Crain, Structure and elasticity of MgO at high pressure, *Am. Mineral.*, **82**, 52-61, 1997a.
- Karki, B. B., L. Stixrude, S. J. Clark, M. C. Warren, G. J. Ackland, and J. Crain, Elastic properties of orthorhombic MgSiO<sub>3</sub> perovskite at lower mantle pressures, *Am. Mineral.*, **82**, 635-638, 1997b.
- Kumazawa, M., and O. L. Anderson, Elastic moduli, pressure derivatives, and temperature derivatives of single-crystal olivine and single-crystal forsterite, *J. Geophys. Res.*, **74**, 5961-5972, 1969.
- Li, B., G. D. Gwanmesia, and R. C. Liebermann, Sound velocities of olivine and beta polymorphs of Mg<sub>2</sub>SiO<sub>4</sub> at earth's transition zone pressures, *Geophys. Res. Lett.*, **23**, 2259-2262, 1996.
- Nielsen, O. H. and R. Martin, Quantum mechanical theory of forces and stresses, *Phys. Rev. B*, **32**, 3780-3788, 1985.
- Tanimoto, T. and D. L. Anderson, Mapping convection in the mantle, *Geophys. Res. Lett.*, **11**, 287-290, 1984.
- Troullier, N. and J. L. Martins, Efficient pseudopotentials for plane-wave calculations. *Phys. Rev. B*, **43**, 1993-2003, 1991.
- Walck, M. C., The P-wave upper mantle structure beneath an active spreading centre: the Gulf of California, *Geophys. J. Roy. Astr. Soc.*, **76**, 697-723, 1984.
- Walck, M. C., The upper mantle beneath the north-east Pacific rim: a comparison with the Gulf of California, *Geophys. J. Roy. Astr. Soc.*, **81**, 243-276, 1985.
- Wentzcovitch, R. M., Invariant molecular dynamics approach to structural phase transitions, *Phys. Rev. B*, **44**, 2358-2361, 1991.
- Wentzcovitch, R. M., J. L. Martins, and G. D. Price, *Ab initio* molecular dynamics with variable cell shape: application to MgSiO<sub>3</sub> perovskite, *Phys. Rev. Lett.*, **70**, 3947-3950, 1993.
- Wentzcovitch, R. M., D. A. Hugh-Jones, R. J. Angel, and G. D. Price, *Ab Initio* study of MgSiO<sub>3</sub> C2/c enstatite, *Phys. Chem. Minerals*, **22**, 453-460, 1995.
- Wentzcovitch, R. M., and L. Stixrude, Crystal chemistry of forsterite: a first principles study, *Am. Mineral.*, (in press) (1997).
- Yoneda, A. and M. Morioka, Pressure derivatives of elastic constants of single crystal forsterite, in *High Pressure Research: Applications to Earth and Planetary Sciences*, Y. Syono and M. H. Manghnani, eds., pp. 207-213, Terra Scientific, Tokyo, 1992.
- Zaugg, J. M., E. H. Abramson, J. M. Brown, and L. J. Slutsky, Sound velocities in olivine at earth mantle pressures, *Science*, **260**, 1487-1489, 1993.
- Zha, C. S., T. S. Duffy, R. T. Downs, H. K. Mao, Sound velocity and elasticity of single-crystal forsterite to 16 GPa, *J. Geophys. Res.*, **101**, 17535-17545, 1996.

C. da Silva and R. M. Wentzcovitch, Dept. of Chemical Engineering and Materials Science, University of Minnesota, Minneapolis, MN 55455

L. Stixrude, School of Earth and Atmospheric Sciences, Georgia Institute of Technology, Atlanta, GA 30332-0340.

(Received April 23, 1997; accepted June 7, 1997.)